Atmos. Meas. Tech., 6, 927–936, 2013
www.atmos-meas-tech.net/6/927/2013/
doi:10.5194/amt-6-927-2013

Atmospheric Measurement Techniques
Open Access

Selective measurements of NO, NO_2 and NO_y in the free troposphere using quantum cascade laser spectroscopy

B. Tuzson[1], K. Zeyer[1], M. Steinbacher[1], J. B. McManus[2], D. D. Nelson[2], M. S. Zahniser[2], and L. Emmenegger[1]

[1]Empa, Swiss Federal Laboratories for Materials Science and Technology, Laboratory for Air Pollution and Environmental Technology, Überlandstr. 129, 8600 Dübendorf, Switzerland
[2]Aerodyne Research, Inc., Center for Atmospheric and Environmental Chemistry, Billerica, MA 01821, USA

Correspondence to: B. Tuzson (bela.tuzson@empa.ch)

Received: 11 December 2012 – Published in Atmos. Meas. Tech. Discuss.: 20 December 2012
Revised: 8 March 2013 – Accepted: 19 March 2013 – Published: 9 April 2013

Abstract. A quantum cascade laser based absorption spectrometer for continuous and direct measurements of NO and NO_2 was employed at the high-altitude monitoring site Jungfraujoch (3580 m a.s.l., Switzerland) during a three-month campaign in spring/summer 2012. The total reactive nitrogen, NO_y, was also measured in the form of NO after conversion on a gold catalyst. The aim was to assess the suitability of the instrument for long-term monitoring of the main reactive nitrogen species under predominantly free tropospheric air conditions. A precision (1σ) of 10 and 3 ppt for NO and NO_2 was achieved under field conditions after 180 s averaging time. The linear dynamic range of the instrument has been verified for both species from the detection limit up to 45 ppb. The spectrometer shared a common sampling inlet with a chemiluminescence-based analyzer. The comparison of the time series shows excellent agreement between the two techniques and demonstrates the adequacy of the laser spectroscopic approach for this kind of demanding environmental applications.

1 Introduction

In the troposphere, the abundance of reactive nitrogen species is primarily influenced by emissions from anthropogenic sources in the form of nitrogen oxides (NO_x = NO + NO_2). Once in the atmosphere, these species are involved in a number of different chemical pathways and oxidized to a large variety of other reactive nitrogen species denoted as NO_y (Crutzen, 1979; Logan, 1983). Despite their low atmospheric concentrations, nitrogen oxides represent an important factor regarding air quality given their contribution to local ozone production and secondary organic aerosol formation. Furthermore, the adverse effect of NO_2 on the human respiratory system and the formation of nitric acid (HNO_3), which is the dominant sink of NO_x (via dry and wet deposition), makes it a harmful air pollutant (Wesely and Hicks, 2000; Jacob, 2000). The significance of NO_x in tropospheric chemistry triggered the interest in instrumental development. This is a challenging task given the substantial spatial and temporal variability of NO_x, which ranges from a few ppt at remote locations to > 100 ppb in urban regions. Nevertheless, it has been addressed over the last two decades by a wide variety of measurement techniques and by even larger number of instrumentations (e.g., see review by Clemitshaw, 2004 and references therein). Although recent intercomparison studies demonstrate that several techniques perform well (Fehsenfeld et al., 1990; Fuchs et al., 2010), they still involve research grade instruments that are not yet established as routine monitoring tools.

At present, chemiluminescence detection (CLD) can be considered as the standard technique, which is routinely used in field missions and air quality monitoring (Demerjian, 2000; GAW Report #195, 2011). Although the method has very good precision for NO, it is unable to directly measure NO_2. Nevertheless, this has successfully been overcome by including the catalytic or photolytic conversion of NO_2 to NO prior to analysis. Besides the necessity of systematic determination of the conversion efficiency, the conversion may also lead to interferences of other nitrogen compounds that can readily be converted to NO (Dunlea et al., 2007; Steinbacher et al., 2007), possibly resulting in overestimated NO_2

readings. The alternating measurement of NO and NO_x can also lead to artifacts in the NO_2 determination when the ambient NO_x levels experience rapid changes. Thus, a setup with two individual CLDs (three in case of NO, NO_x and NO_y observations) is the preferred – but not inexpensive – configuration.

For the present study, we adopted the dual laser design approach recently reported by McManus et al. (2010). Our choice for quantum cascade laser based direct absorption spectroscopy (QCLAS) was driven by two major factors: (i) our previous campaigns performed in a large variety of environments including grassland, forest and mountain sites (Tuzson et al., 2008, 2011; Neftel et al., 2010; Kammer et al., 2011) showed that QCLAS is a robust and reliable technique to be employed under various field and measurement conditions, and (ii) we obtained up to date the longest (more than four years of continuous operation) time series of CO_2 isotope ratio measurements at a mountain site, which reflects the sturdy operation capability of the QCLs (Sturm et al., 2013). In addition to these considerations, the direct absorption technique offers a simple and straightforward solution to perform absolute spectroscopic quantification of the molecular species of interest.

In the following sections we describe the laser instrument, the measurement strategy and the experimental setup used for the campaign to perform direct and simultaneous measurements of NO and NO_2. The validation of the time series recorded during three months of continuous operation is done against the standard CLD method. A short discussion is given on the discrepancy seen when employing the catalytic gold converter for NO_y measurements.

2 Experimental

2.1 Instrumentation

2.1.1 NO_x QCLAS

The spectroscopic instrument (Aerodyne Research, Inc., USA) employed in this study is based on continuous wave quantum cascade laser (cw-QCL) technology. A recent review on optical design, performance characteristics and application fields of this kind of analyzer has been presented by McManus et al. (2010). Briefly, the spectrometer embodies two room-temperature cw-QCLs (Alpes Lasers, Switzerland) emitting in the spectral range of 1600 and 1900 cm^{-1}, respectively. The individual laser beams are first collected by a pair of reflective objectives then combined and co-oriented by a dichroic mirror (LohnStar Optics, Inc., USA) and sent through a wedged beam splitter that results in three different beams. The main beam is further shaped by a series of reflective optics and coupled into an astigmatic Herriott multipass absorption cell (AMAC-200), which folds the laser radiation for a total number of 434 reflections. This results in an effective path length of 204 m (McManus et al., 2011). When the exit condition of the cavity is fulfilled, the laser beam leaves the cell through the same entrance hole and is then focused on a thermoelectrically cooled IR detector (Vigo Systems, Poland). The fraction of the laser beam reflected from the first surface of the beam splitter is directed through a short (5 cm) cell filled with a 1 : 1 mixture of NO and NO_2 and subsequently aimed onto a second detector. This reference path assures the locking of the laser frequency to well-defined absorption lines even in situations when the ambient NO_x concentrations drop below the limit of detection or when the multipass cell is filled with NO_x-scrubbed air for spectral background measurements. The third beam reflected from the back surface of the wedge is used for accurate frequency tuning rate determination of the lasers by placing a germanium etalon in its path. This beam is also focused onto the reference detector. A flipping mechanism selects between the two beams (reference cell or etalon).

Beside the optical assembly design, the electronics have also experienced some major improvements. A significant reduction of the hardware size has been achieved by using compact USB-based data acquisition cards (NI USB-6251 OEM, National Instruments, Inc., USA) and embedded mini-PCs. Low noise laser drivers (Wavelength Electronics, Inc., USA) combined with dedicated power-supply design and thermal management led to unprecedented stability. Details regarding the laser control and spectral fitting software (TDLWintel, Aerodyne Research, Inc., USA) have been discussed previously (Nelson et al., 2004).

Overall, the spectrometer consisted of two full-size 19-inch modules (6U) incorporating optics and electronics, respectively. These units were built into a rack together with the custom-made gas handling and calibration module (3U), a UPS (2U, APC Smart series) to bridge short power outages, and a rack-mount thermoelectric liquid chiller (4U, Thermorack 300, Solid State Cooling Systems) used for cooling the lasers, IR-detectors and temperature stabilizing the optical module. The total weight, including the vacuum pump, of the setup was 175 kg and its power consumption approximately 0.8 kW.

The major advantage of a direct spectroscopic detection of NO_2 is the immunity from interferences associated with photochemical conversion of NO_2 to NO prior to detection. However, this technique may suffer from interferences of other nature, such as overlapping absorption features from other molecular species or pressure broadening effects mainly due to water (Tuzson et al., 2010). Therefore, we performed a detailed investigation of the simulated absorption spectra, generated based on typical experimental parameters and the HITRAN database (Rothman et al., 2009), in the range of 1600 and 1900 cm^{-1}, where NO_2 and NO have their fundamental ro-vibrational modes. The aim was to select the strongest absorption lines possible with the stringent condition that the spectral interferences from water vapor or other trace gases are minimal. The best compromises

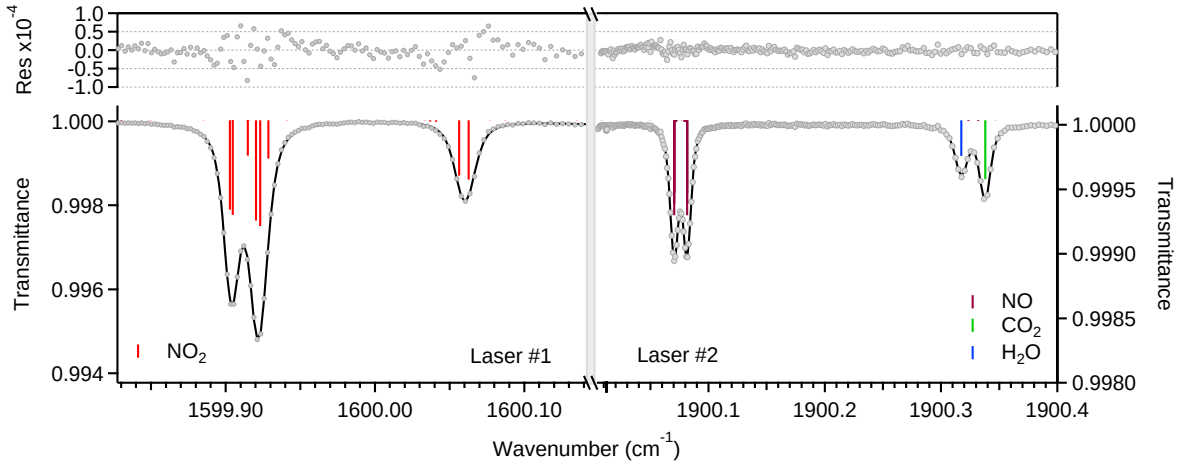

Fig. 1. The selected spectral windows with the absorption lines of NO and NO_2 as measured in ambient air with the dual-laser spectrometer with a multi-pass cell of 204 m path-length at 50 hPa sample pressure. The gray circles indicate measurement points, while the black line is a least-square fit to the data. The residual is shown in the top panel. The colored sticks indicate individual absorption lines of molecules that absorb within the scanning range of the lasers.

we could identify were the doublet lines located at 1900.0706 and 1900.0816 cm^{-1} for NO and the group of lines in the vicinity of 1599.9 cm^{-1} for NO_2 (see Fig. 1). Simulations of typical real-time scenarios involving low NO_x concentrations and various humidity levels indicated low interference effects (< 70 ppt NO_x per volume % H_2O), which was later confirmed experimentally. Based on these examinations, two cw-QCLs were selected correspondingly with single mode emission powers higher than 10 mW at the specified wavelengths. The tuning range of the lasers was chosen such that it also included a water vapor absorption line (Fig. 1). Thus, the air sample humidity could be measured continuously together with the NO_x species, which allowed for analysis and correction of water-related effects.

The instrumental precision has been enhanced by addressing the issue of interference fringes. These are mainly produced by scattered light within the multipass cell and may significantly limit the achievable SNR improvement available from multipass cells. They typically generate an absorption equivalent noise level of 10^{-4} in the background signal. A significant improvement was obtained by careful investigation and selection of circulation patterns that minimize fringes near the absorption line-width and by using high-reflectivity mirrors that lead to lower fringes by reducing the ratio of scattered light to transmitted light (McManus et al., 2011). In addition, a mechanical modulation (dithering) of the cell mirrors by a piezo-crystal helps to average out fringes. As a result, a precision of $\sigma_{min} = 1$ ppt for NO_2 after 12 min of averaging was achieved in the laboratory. Under field conditions, however, this performance may suffer from environmental influences. Therefore, the instrument's stability was investigated on-site by measuring NO_x-free air for a time period of 1 h with a detection bandwidth of 1 Hz and calculating the associated Allan variance as a function of averaging time (Werle et al., 1993). This two-sample variance-plot is shown in Fig. 2 and allows defining the optimum calibration time scale. The variance curve reveals flicker noise contributions to the signal, manifested as deviations from the expected $1/\tau$ slope, at around 10 and 220 s. Similar behavior has been described by Werle (2011) and associated to optical fringes. Following his theoretical framework, it was possible to closely reproduce the observed deviations by assuming two periodic fringe components with frequencies of 4.3×10^{-2} Hz and 2.2×10^{-3} Hz, respectively. In fact, the 23 s periodicity correlates well with the PID-cycle of the temperature controller employed for stabilizing the optical module. The slow fringe is probably due to opto-mechanical drifts or variations in the driver electronics, reflecting the temperature fluctuations (±2 °C) experienced at the monitoring station. Nevertheless, the precision achieved at the monitoring site after 180 s averaging time was 3 and 10 ppt, which corresponds to an absorbance noise level of 5.9×10^{-6} and 8.8×10^{-6} for NO_2 and NO, respectively. Normalizing to the 204 m optical path-length, this corresponds to an absorbance per unit path length sensitivity of 5×10^{-10} cm^{-1}.

The strategy to cope with the drift issue was the frequent and periodic background (zero air) spectrum subtraction from the measured spectrum. Therefore, a cost-effective NO_x filter that consists of a stainless-steel container (1 L) filled with grained activated charcoal (Merck KGaA, Germany) was used to generate NO_x-scrubbed air for spectral background measurements. The NO_x filter efficiency and potential systematic errors, when using the NO_x scrubber for background definition, have been verified by comparing the values measured for ambient air through the filter with data obtained when directly measuring high purity (5.5) He and N_2. As minor differences (< 30 ppt) were observed, we decided to check the NO_x scrubber efficiency during the

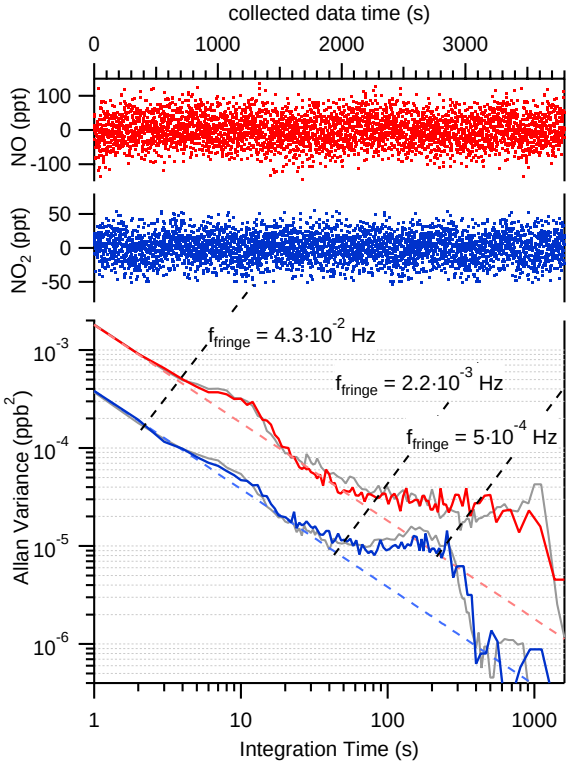

Fig. 2. Allan variance plots for NO and NO_2 measured with the dual-laser instrument at the Jungfraujoch using NO_x-free air as gas sample. The gray lines correspond to calculated white noise plus fringes (f_{fringe}) contributing as flicker noise (details in text).

campaign at every 2 h against N_2. The filter solution was the preferred method over the use of dry N_2 as zero air, because the NO_x filter does not significantly alter the water vapor mixing ratio of the air flowing through it, and thus the zero air better reconciles the sampled air humidity and contributes in reducing possible detection artifacts that could be induced by spectral interferences due to water absorption lines. The most efficient method to maintain the best stability and accuracy of the spectrometer has been achieved by automatically recording a background spectrum every 10 min and subtracting it from each subsequent sample spectrum before fitting. Uncertainties due to background drifts, mainly caused by temperature fluctuations, can be significant (> 40 ppt), if no action is taken. However, the configuration of the measurement cycle, as we have used in the field mission, allowed in the post-processing step to minimize these uncertainties. Their contributions to the 10 min averaged values were estimated to 5 ± 4 ppt for NO_2 and 11 ± 7 ppt for NO. More details about the measurement cycle and data analysis are presented in the Sect. 3.

2.1.2 Chemiluminescence NO_x detection

The routine, long-term monitoring of NO, NO_x and NO_y at the Jungfraujoch is performed with commercially avail-

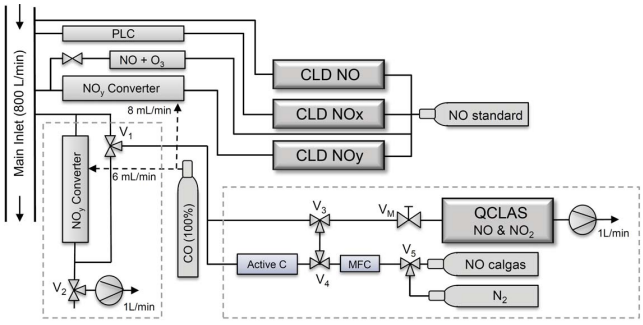

Fig. 3. Experimental setup at Jungfraujoch. The equipment within the dashed boxes was operated for a three-month period, while the other instrumentation is part of the permanent monitoring program.

able chemiluminescence analyzers (CraNOx, Eco Physics, Switzerland). The chemiluminescence detection (CLD) technique, developed in the 1970s, is the reference method recommended by the US EPA (Demerjian, 2000) and by European legislation (European Standard, EN 14211, 2012) for the measurement of NO_x in monitoring networks. The method relies on the light emission from the electronically excited NO_2, a product generated in the gas-phase reaction of ambient NO with O_3 added in excess to the air sample. The emission intensity is directly proportional to the concentration of NO in the air, and the emitted photons are detected by a photomultiplier tube. NO_x is measured as NO after photolytic conversion of NO_2. The atmospheric NO_2 is then derived by subtraction of NO from the NO_x signal (Ridley and Howlett, 1974; Ryerson et al., 2000; Sadanaga et al., 2010). NO_y species are converted to NO on a heated gold catalyst (300 °C) in the presence of CO as a reducing agent (Fahey et al., 1985).

The measurement procedure as well as the calibration strategy has repeatedly been described in detail (Zellweger et al., 2000; Pandey Deolal et al., 2012). Here we just recall that, for the sensitive measurement of the NO–NO_x–NO_y species, three dedicated CLDs are used. The detection limits of the CLDs for NO and NO_y after 2 min averaging are 20 ppt, whereas it is 50 ppt for the NO_2 channel due to the incomplete conversion and the determination of NO_2 by the difference of two measured (NO and NO + converted NO_2) signals. The overall measurement uncertainty (1σ) is 9 % for NO_y and 5 % for NO_x, including CLD precision, the NO standard uncertainty, and the conversion efficiencies of the photolytic convertor (PLC). Data are processed and reported as 10 min averages.

Since the PLC–CLD setup is used as the standard method, these measurements are taken as reference for validating the QCLAS data.

2.2 Site description and sampling setup

Field measurements took place between 22 March and 25 June 2012 at the high alpine research station Jungfraujoch (JFJ, 46.55 ° N, 7.98 ° E , elevation 3580 m). The monitoring station is one of the 28 global sites of the Global Atmosphere Watch (GAW) program of the World Meteorological Organization (WMO). Given its location, the air sampled here is expected to be representative for the lower free troposphere over Europe, which is mainly the case in the autumn and winter season, while in late spring and summer it can be influenced by the planetary boundary layer (Baltensperger et al., 1997; Lugauer et al., 1998; Zellweger et al., 2003). Long-term continuous in situ monitoring of trace gases such as NO, NO_2, NO_y, CO, and O_3 is routinely performed by Empa within the activities of the Swiss National Air Pollution Monitoring Network (NABEL).

The ambient air was sampled using the monitoring site's heated stainless steel main inlet (inner diameter 9 cm) situated about 3 m above ground, in which the ambient air is drawn at a high flow rate of $> 800\,\mathrm{L\,min^{-1}}$ (Fig. 3). The main manifold is temperature controlled to keep the gas temperature at its lower end at constant 10 °C. Potential losses of NO_y in the sampling lines were minimized by placing the gold converter close to the main inlet, connected with about 1 m long PFA tubing. The time required for the air to reach the converter was about 2 s. The photolytic converter (PLC 762, Eco Physics, Switzerland) for the NO_2 measurement was placed next to the NO_y converter. Downstream of the converters, the air is drawn through separate PFA tubing to the chemiluminescence analyzers. The air for the NO analysis is drawn directly from the main manifold with PFA tubing.

The NO analyzers are automatically calibrated every 39 h by measuring zero air and NO standard gas (5 ppm NO in N_2, referenced against NIST Standard Reference Material (SRM 2629a) and NMI Primary Reference Material (PRM BD11)) diluted with zero air to approximately 48 ppb. The conversion efficiency of the converter is determined by gas phase titration of NO with ozone every 78 h. The conversion efficiency of the PLC usually ranged from 74 to 58 %.

The QCLAS was operated alongside the CLDs for the duration of the study. An additional gold converter (CON 765, Eco Physics, Switzerland) was mounted next to the NABEL NO_y converter and shared the same CO source (purity 99.997 %, Messer-Griesheim GmbH), whereas the sampling line was independently connected to the main inlet. The selection between ambient air and air passing through the gold converter was accomplished by a 3-way all-Teflon solenoid valve (Teqcom Ind., USA). The flow rate of $1\,\mathrm{L\,min^{-1}}$ was manually adjusted by a PTFE needle valve V_M (PKM, Switzerland) mounted upstream of the cell (see Fig. 3), while the cell pressure ($\simeq 50$ hPa) was established by selecting the appropriate pumping rate with an integrated potentiometer on the oil-free diaphragm pump (N920 series, KNF, Germany). Measurements were done continuously at 1 s time resolution and post-processed to meet the 10 min averaging time scale of the CLD.

3 Results and discussion

For free tropospheric air composition monitoring, high instrumental precision alone is not sufficient to obtain the necessary accuracy. In fact, an optimal calibration and sampling strategy is equally important and has a decisive influence on the data quality. The strategy employed in this study exploits the very high precision and the fast response of the instrument when measuring zero air, and it accounts for drifts that may dominate the system at longer time scales. It consists of various steps repeated in half-hour sequence. First, a background spectrum is recorded using NO_x-scrubbed air as described in the previous section. This is achieved by directing the sampled ambient air through the NO_x filter by switching the solenoid valve V_3 (see Fig. 3) and purging the absorption cell for 120 s. The last 10 s are then averaged and used to determine the spectral baseline and perform a background correction by subtracting it from all the subsequent spectra. The second step involves measuring NO and NO_2 simultaneously for 10 min by drawing sample air directly through the absorption cell. In the next step, the solenoid valve V_1 is switched together with V_2 to divert the air flow across the gold converter, and thus the NO_y mixing ratio is measured as NO during another 10 min. The NO_2 signal can later be used to verify the converter efficiency for NO_2 or to monitor baseline changes due to humidity variations or potential instrumental drifts. After a 20 min measurement period, the system is switched back to measure zero air again, followed by another background definition for the next cycle. The Allan variance plot in Fig. 2 suggests that at least two slow fringe components prevent long averaging times by introducing an instrumental drift. This shows up in the time series of the background signal as a linear trend, and averaging over more than 10 min would obviously reduce the measurement accuracy. However, re-measuring the "zero-level" after the ambient air measurements provides a convenient way to monitor the amount of drift. The difference between the latter and initial "zero-level" measurements was considered as real drift in the system, and a linear interpolation between the two values was used to correct the 1 s measurement values within this interval prior to averaging. For more confidence in the "absolute" zero baseline determination, dry N_2 from a gas cylinder (purity 5.5) was measured instead of NO_x-scrubbed air every 2 h. This acts as an additional parameter for monitoring the performance of the NO_x filter and to correct the NO_x data for systematic offsets. Over the whole campaign, the N_2 measurements showed slightly lower NO (-32 ± 15 ppt) and slightly higher NO_2 (15 ± 9 ppt) values than the NO_x-scrubbed air. Although nearly negligible, the values were included as offset correction for the QCLAS data. Moreover,

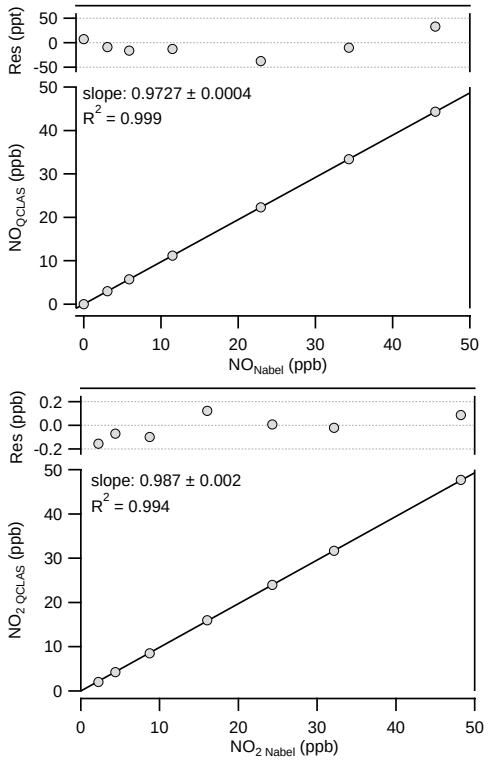

Fig. 4. Calibration plots of the QCLAS data for NO and NO_2. The abscissa represents the values determined from standard gas dilution (details in text). The fit (black line) is determined by weighted orthogonal distance regression and its residual shown in the upper part of each plot.

it also aided in establishing the water-vapor-induced interferences, which were applied to correct the measurement values. The amount of this correction was empirically determined as being -16.8 ± 3.7 ppt NO and -57.3 ± 3.5 ppt NO_2 for 1 % volume H_2O. The relative humidity (RH) at JFJ varied between 20 and 100 %, depending on meteorological conditions and wind directions, but predominantly ($\simeq 87$ % of all values) it was above 75 % RH. During the campaign, the temperature gradually increased from -11 °C (in March) to around 0 °C (in June), while the air pressure remained rather constant at 654 ± 8 hPa. The water vapor was below 0.3 % during the whole campaign, and thus its effect was rather marginal, leading to a minor correction only (i.e., 5 to 20 ppt in the measured NO and NO_2 values). Since the water vapor corrections of the NO_x data are based on the spectroscopically measured H_2O values, potential lag times have no influence on the data quality.

Dynamic dilutions of standard NO_2 (96.3 ± 3.7 ppb) and NO (5 ± 0.1 ppm) gases were used to establish the span of the laser spectrometer for the NO_x measurements from the detection limit up to 50 ppb, and to calibrate the raw spectroscopic data against the standard scale used by NABEL (see Fig. 4 and previous section). The accuracy of this calibration is dominated by the accuracy of the mass flow controllers (MFCs) used for the dilution. These MFCs (red-y smart series, Voegtlin, Switzerland) were referenced against a high-accuracy venturi flowmeter (molbloc, DH Instruments/Fluke, USA) at Empa. The estimated uncertainties resulted from the dilution process were 0.1 % and 0.4 % for NO and NO_2, respectively. Since NO_2 gas mixtures in cylinders are known to be unstable, the NO_2 concentration was first determined with a calibrated CLD followed by QCLAS measurements and dynamic dilution (Fig. 4). The sampling line was taken the same, and thus we assumed that losses of NO_2 on the metallic surfaces of the pressure regulator and MFCs are similar. Obviously, the total uncertainty in this case is mainly given by systematic errors due to losses. To summarize, the total uncertainty of the QCLAS at large NO_x values is determined by the accuracy of the calibration gases, which lies in the percent range ($\pm$2–4 %), while at sub-ppb levels it is mainly given by the uncertainty of the "zero-level" measurements, which is below 10 ppt.

Finally, it is noted that all parameters discussed above were determined on the monitoring station at JFJ. This assured a direct link to the retrieved tropospheric NO_x data. Figure 5 shows an exemplary window of 21 days from the time series recorded by both techniques during the campaign. The challenge of such tropospheric air measurements is well illustrated by the NO data, where ~ 78 % of the values are below 0.1 ppb. Despite of this, the variations in the mixing ratio profiles of NO and NO_2 compare very well between the CLD and the QCLAS. The quantitative agreement is illustrated in Fig. 6 in the form of correlation plots and the associated regression results for NO_x and NO_y measured over the three-month mission. For the analysis, we employed the orthogonal distance regression method, which includes the errors in both dependent and independent variables (X- and Y-values) as well as the weighting with the expected magnitude of errors for each individual data point. The calibrated QCLAS data were averaged to 10 min (600 points) to match the time resolution of the CLD, and the error of the mean of each individual averaged value was used to filter out those data points that exhibited too large (3σ of the CLD detection limit) variations. This minimized the scatter due to synchronization and time response differences between instruments in situations where the NO_x concentrations changed abruptly during the averaging time interval. Statistical analysis on the differences between all NO_x data reported by the two analyzers showed that more than 94 % of individual data points agreed to within $\pm$50 ppt and were included for the regression analysis (Fig. 6).

In the case of the NO_y time series, we observed a systematic discrepancy of about 0.26 ppb, which, over the measurement period, displayed short-term (< 12 h) variations of up to 1.2 ppb. Additional tests, involving different gases (ambient air, dry N_2 and diluted NO standard) as common input sample to the converters and alternating measurements with QCLAS and CLD, revealed that the two converters

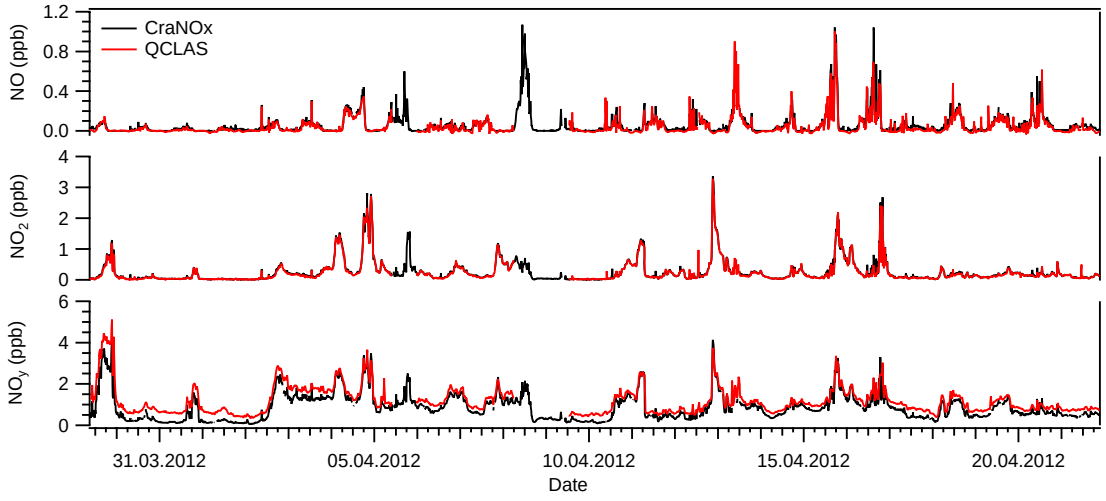

Fig. 5. An exemplary sequence of NO, NO_2 and NO_y time series measured at the Jungfraujoch with the two different methods. Note the different scaling of the y-axis. The gaps in the QCLAS data were caused by additional on-site works, such as calibration and converter investigation (see details in text).

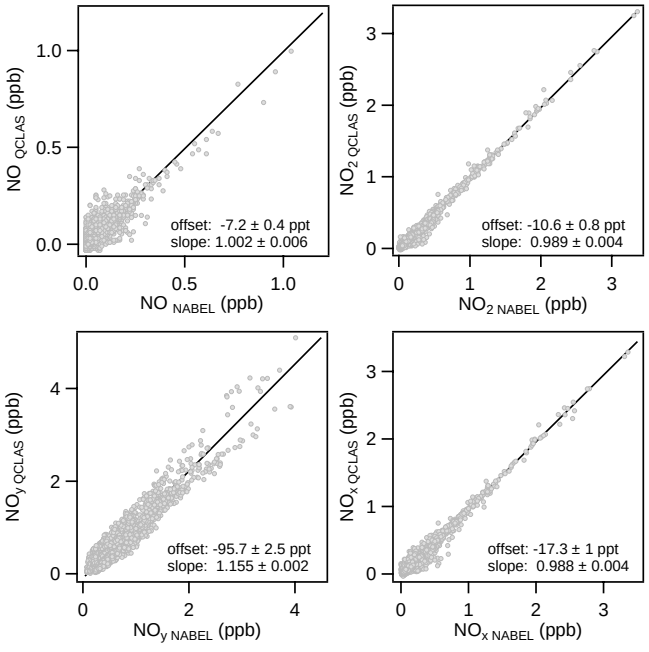

Fig. 6. Correlation plots of the QCLAS and CraNOx data. The results of the regression analysis are given as slope and intercept values.

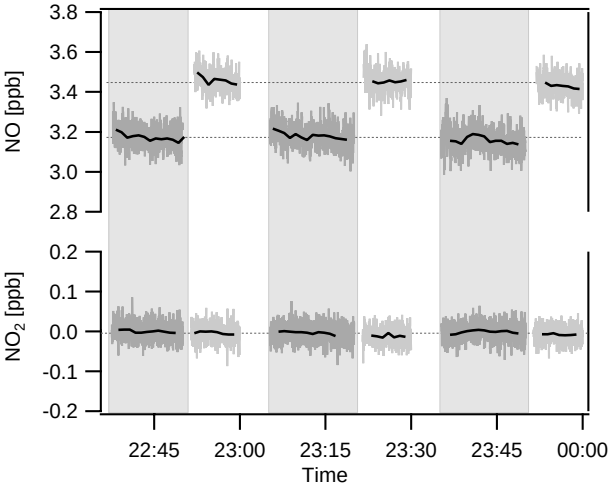

Fig. 7. NO and NO_2 mixing ratios measured with the QCLAS when switching between the two gold converters measuring NO standard gas diluted with "zero" air. The gray areas correspond to the measurements of the converter used by the NABEL monitoring instrumentation.

generate indeed different amounts of NO_y in good agreement with the discrepancy seen for the time series. Figure 7 shows the clear bias seen by the QCLAS when switching between the two Au converters sharing the same inlet with diluted NO standard as sample gas. The difference disappeared only when dry N_2 was flowing through the converters. This analysis eliminates suspected issues related to CLD technique (i.e., quenching, O_3 and H_2O effects), as it shows that the difference still exists when alternating the converters and analyzing the NO_y directly with the QCLAS. Therefore, the mismatch between the two gold converters has fully been attributed to their slightly different conversion efficiencies. Even though, for NO_2, the converters' efficiencies were found comparable (within 98.5 %), Au catalyst may have different efficiencies for the various reactive nitrogen species or may suffer from contributions of other interfering compounds. According to systematic investigations, species such as nitric acid (HNO_3) and peroxyacyl nitrates (PANs) can have conversion efficiencies up to 95 %, whereas ammonia

(NH_3) and hydrogen cyanide (HCN) in the presence of water vapor show little but variable contribution (1–5 %), and their magnitude depends on the surface history and temperature of the converter (Kliner et al., 1997; Fahey et al., 1985; Volz-Thomas et al., 2005). Although we had no speciation measurements for these compounds, literature data allow for an estimate of their contribution. Partitioning measurements of NO_y in the lower free troposphere (Zellweger et al., 2003) revealed that PAN is the dominant NO_y species ($\sim$ 38 %) during spring, followed by inorganic nitrate (HNO_3 (7 %) and particulate nitrate (17 %)). Mixing ratio values of $\sim$ 200 ppt for HCN at the JFJ were reported by Rinsland et al. (2000). Considering the above values and assuming that the conversion efficiency of the thermally unstable PAN in the gold converter should be very similar to the conversion efficiency for NO_2, the observed mismatch between the converters remains unclear. Interestingly, we also observed a significant difference in the CO_2 content of the gas samples after the converters, despite the similar CO flow rates (see Fig. 3). While the CO_2 level remained unchanged after passing through the converter with lower NO_y values, the other converter almost doubled the amount of CO_2. Further investigation of the NO_y data revealed that the temporal variability of its relative difference closely follows the humidity fluctuations in the ambient air. The observed discrepancies in NO_y were systematically becoming larger when the relative humidity dropped below 70 %. This may well be caused by issues related to HNO_3 such as conversion efficiency of the gold converter, memory effects or inlet transmission efficiencies, but at the present we have no plausible explanation for this behavior. Finally, it should be noted that slightly lower NO_y values (6–10 %) in the NABEL system have already been observed during intercomparison campaigns (Zellweger et al., 2003; Pandey Deolal et al., 2012), and were attributed to potential losses of HNO_3 in the inlet system. This probably has to be reconsidered, and further investigations of Au converters as well as their regular comparisons are recommended for assessing the data quality.

4 Conclusions

The validation and long-term performance assessment of a quantum cascade laser spectrometer was successfully accomplished at the high-altitude research station JFJ by measuring the tropospheric NO_x and NO_y mixing ratios accompanied by standard monitoring CLD technique. To our knowledge, this is the first intercomparison study of this kind, involving a laser absorption technique for direct and simultaneous measurement of both NO and NO_2, under field conditions. The time series recorded with QCLAS show very good correlation with the CLD data even at sub-ppb mixing ratio levels. A dedicated gas sampling/handling method combined with the high instrumental precision (< 10 ppt) delivered the accuracy and drift suppression needed for reliable background tropospheric air NO_x monitoring. Since both techniques give similar results, there is no fundamental reason to replace the well-established and reliable CLD technique by QCLAS. Nevertheless, the possibility to detect NO_2 selectively that is, without chemical conversion, and with high time resolution (1 Hz) is very attractive. Furthermore, significant advances in quantum cascade laser technology let us anticipate the appearance of compact multi-color sources, which would lead to substantial simplification of the optical design resulting in more robust, compact, and cost-effective analyzers.

The intercomparison of the NO_y data revealed differences that could not be attributed to any of the measurement techniques, but rather were associated with the conversion efficiency of the gold catalyst. This was confirmed in a dedicated set of experiments, but the exact reason for the different behavior of the two seemingly identical catalysts remains unclear. Obviously, there are limitations of the existing NO_y method, which may require the development of more robust conversion schemes or, preferably, measurement techniques for compound-specific determination of the NO_y species.

Acknowledgements. This work was supported by the Federal Office for the Environment (FOEN), Switzerland and the Swiss National Science Foundation (SNSF/R'Equip). We thank the International Foundation High Altitude Research Stations Jungfraujoch and Gornergrat (HFSJG) for access to the facilities at the Research Station Jungfraujoch and the custodians for on-site support. Beat Schwarzenbach (Empa) is acknowledged for calibrating our NO_2 working standard. We also acknowledge the valuable contributions of Ryan McGovern, Stanley Huang and Michael Agnese (ARI).

Edited by: P. Werle

References

Baltensperger, U., Gäggeler, H. W., Jost, D. T., Lugauer, M., Schwikowski, M., Weingartner, E., and Seibert, P.: Aerosol climatology at the high-alpine site Jungfraujoch, Switzerland, J. Geophys. Res.-Atmos., 102, 19707–19715, doi:10.1029/97JD00928, 1997.

Clemitshaw, K. C.: A review of instrumentation and measurement techniques for ground-based and airborne field studies of gas-phase tropospheric chemistry, Crit. Rev. Env. Sci. Tec., 34, 1–108, doi:10.1080/10643380490265117, 2004.

Crutzen, P. J.: The role of NO and NO_2 in the chemistry of the troposphere and stratosphere, Annu. Rev. Earth Pl. Sc., 7, 443–472, doi:10.1146/annurev.ea.07.050179.002303, 1979.

Demerjian, K. L.: A review of national monitoring networks in North America, Atmos. Environ., 34, 1861–1884, doi:10.1016/S1352-2310(99)00452-5, 2000.

Dunlea, E. J., Herndon, S. C., Nelson, D. D., Volkamer, R. M., San Martini, F., Sheehy, P. M., Zahniser, M. S., Shorter, J. H., Wormhoudt, J. C., Lamb, B. K., Allwine, E. J., Gaffney, J. S., Marley, N. A., Grutter, M., Marquez, C., Blanco, S., Cardenas, B., Retama, A., Ramos Villegas, C. R., Kolb, C. E.,

Molina, L. T., and Molina, M. J.: Evaluation of nitrogen dioxide chemiluminescence monitors in a polluted urban environment, Atmos. Chem. Phys., 7, 2691–2704, doi:10.5194/acp-7-2691-2007, 2007.

Fahey, D. W., Eubank, C. S., Hubler, G., and Fehsenfeld, F. C.: Evaluation of a catalytic reduction technique for the measurement of total reactive odd-nitrogen NO_y in the atmosphere, J. Atmos. Chem., 3, 435–468, doi:10.1007/BF00053871, 1985.

Fehsenfeld, F. C., Williams, E. J., Buhr, M. P., Hübler, G., Langford, A. O., Murphy, P. C., Parrish, D. D., Norton, R. B., Fahey, D. W., Drummond, J. W., Mackay, G. I., Roychowdhury, U. K., Hovermale, C., Mohnen, V. A., Demerjian, K. L., Galvin, P. J., Calvert, J. G., Ridley, B. A., Grahek, F., Heikes, B. G., Kok, G. L., Shetter, J. D., Walega, J. G., Elsworth, C. M., and Schiff, H. I.: Intercomparison of NO_2 measurement techniques, J. Geophys. Res., 95, 3579–3597, doi:10.1029/JD095iD04p03579, 1990.

Fuchs, H., Ball, S. M., Bohn, B., Brauers, T., Cohen, R. C., Dorn, H.-P., Dubé, W. P., Fry, J. L., Häseler, R., Heitmann, U., Jones, R. L., Kleffmann, J., Mentel, T. F., Müsgen, P., Rohrer, F., Rollins, A. W., Ruth, A. A., Kiendler-Scharr, A., Schlosser, E., Shillings, A. J. L., Tillmann, R., Varma, R. M., Venables, D. S., Villena Tapia, G., Wahner, A., Wegener, R., Wooldridge, P. J., and Brown, S. S.: Intercomparison of measurements of NO_2 concentrations in the atmosphere simulation chamber SAPHIR during the NO3Comp campaign, Atmos. Meas. Tech., 3, 21–37, doi:10.5194/amt-3-21-2010, 2010.

GAW Report #195. A WMO/GAW Expert Workshop on Global Long-term Measurements of Nitrogen Oxides and Recommendations for GAW Nitrogen Oxides Network (WMO TD No. 1570), available at: www.wmo.int/pages/prog/arep/gaw/documents/Final_GAW_195_TD_No_1570_web.pdf, 2011.

Jacob, D. J.: Heterogeneous chemistry and tropospheric ozone, Atmos. Environ., 34, 2131–2159, doi:10.1016/S1352-2310(99)00462-8, 2000.

Kammer, A., Tuzson, B., Emmenegger, L., Knohl, A., Mohn, J., and Hagedorn, F.: Application of a quantum cascade laser-based spectrometer in a closed chamber system for real-time $\delta^{13}C$ and $\delta^{18}O$ measurements of soil-respired CO_2, Agr. Forest Meteorol., 151, 39–48, doi:10.1016/j.agrformet.2010.09.001, 2011.

Kliner, D. A. V., Daube, B. C., Burley, J. D., and Wofsy, S. C.: Laboratory investigation of the catalytic reduction technique for measurement of atmospheric NO_y, J. Geophys. Res.-Atmos., 102, 10759–10776, doi:10.1029/96JD03816, 1997.

Logan, J. A.: Nitrogen oxides in the troposphere: global and regional budgets, J. Geophys. Res., 88, 10785–10807, doi:10.1029/JC088iC15p10785, 1983.

Lugauer, M., Baltensperger, U., Furger, M., Gäggeler, H. W., Jost, D. T., Schwikowski, M., and Wanner, H.: Aerosol transport to the high Alpine sites Jungfraujoch (3454 m a.s.l.) and Colle Gnifetti (4452 m a.s.l.), Tellus B, 50, 76–92, doi:10.1034/j.1600-0889.1998.00006.x, 1998.

McManus, J. B., Zahniser, M. S., Nelson, D. D., Shorter, J. H., Herndon, S., Wood, E., and Wehr, R.: Application of quantum cascade lasers to high-precision atmospheric trace gas measurements, Opt. Eng., 49, 111124–111135, doi:10.1117/1.3498782, 2010.

McManus, J. B., Zahniser, M. S., and Nelson, D. D.: Dual quantum cascade laser trace gas instrument with astigmatic Herriott cell at high pass number, Appl. Opt., 50, A74–A85, doi:10.1364/AO.50.000A74, 2011.

Neftel, A., Ammann, C., Fischer, C., Spirig, C., Conen, F., Emmenegger, L., Tuzson, B., and Wahlen, S.: N_2O exchange over managed grassland: Application of a quantum cascade laser spectrometer for micrometeorological flux measurements, Agr. Forest Meteorol., 150, 775–785, doi:10.1016/j.agrformet.2009.07.013, 2010.

Nelson, D. D., McManus, B., Urbanski, S., Herndon, S., and Zahniser, M. S.: High precision measurements of atmospheric nitrous oxide and methane using thermoelectrically cooled mid-infrared quantum cascade lasers and detectors, Spectrochim. Acta A, 60, 3325–3335, doi:10.1016/j.saa.2004.01.033, 2004.

Pandey Deolal, S., Brunner, D., Steinbacher, M., Weers, U., and Staehelin, J.: Long-term in situ measurements of NO_x and NO_y at Jungfraujoch 1998–2009: time series analysis and evaluation, Atmos. Chem. Phys., 12, 2551–2566, doi:10.5194/acp-12-2551-2012, 2012.

Ridley, B. A. and Howlett, L. C.: An instrument for nitric oxide measurements in the stratosphere, Rev. Sci. Instrum., 45, 742–748, doi:10.1063/1.1686726, 1974.

Rinsland, C. P., Mahieu, E., Zander, R., Demoulin, P., Forrer, J., and Buchmann, B.: Free tropospheric CO, C_2H_6, and HCN above central Europe: Recent measurements from the Jungfraujoch station including the detection of elevated columns during 1998, J. Geophys. Res.-Atmos., 105, 24235–24249, doi:10.1029/2000JD900371, 2000.

Rothman, L. S., Gordon, I. E., Barbe, A., Chris Benner, D., Bernath, P. F., Birk, M., Boudon, V., Brown, L. R., Campargue, A., Champion, J. -P., Chance, K., Coudert, L. H., Dana, V., Devi, V. M., Fally, S., Flaud, J. -M., Gamache, R. R., Goldman, A., Jacquemart, D., Kleiner, I., Lacome, N., Lafferty, W. J., Mandin, J. -Y., Massie, S. T., Mikhailenko, S. N., Miller, C. E., Moazzen-Ahmadi, N., Naumenko, O. V., Nikitin, A. V., Orphal, J., Perevalov, V. I., Perrin, A., Predoi-Cross, A., Rinsland, C. P., Rotger, M., Šimečková, M., Smith, M. A. H., Sung, K., Tashkun, S. A., Tennyson, J., Toth, R. A., Vandaele, A. C. and Vander Auwera, J.: The HITRAN 2008 molecular spectroscopic database, J. Quant. Spectrosc. Ra., 110, 533–572, doi:10.1016/j.jqsrt.2009.02.013, 2009.

Ryerson, T. B., Williams, E. J., and Fehsenfeld, F. C.: An efficient photolysis system for fast-response NO_2 measurements, J. Geophys. Res.-Atmos., 105, 26447–26461, doi:10.1029/2000JD900389, 2000.

Sadanaga, Y., Fukumori, Y., Kobashi, T., Nagata, M., Takenaka, N., and Bandow, H.: Development of a selective light-emitting diode photolytic NO_2 converter for continuously measuring NO_2 in the atmosphere, Anal. Chem., 82, 9234–9239, doi:10.1021/ac101703z, 2010.

Steinbacher, M., Zellweger, C., Schwarzenbach, B., Bugmann, S., Buchmann, B., Ordóñez, C., Prevot, A. S. H., and Hueglin, C.: Nitrogen oxide measurements at rural sites in Switzerland: bias of conventional measurement techniques, J. Geophys. Res.-Atmos., 112, D11307, doi:10.1029/2006JD007971, 2007.

Sturm, P., Tuzson, B., Henne, S., and Emmenegger, L.: Tracking isotopic signatures of CO_2 at Jungfraujoch with laser spectroscopy: analytical improvements and exemplary results, Atmos. Meas. Tech. Discuss., 6, 423–459, doi:10.5194/amtd-6-423-2013, 2013.

Tuzson, B., Mohn, J., Zeeman, M. J., Werner, R. A., Eugster, W., Zahniser, M. S., Nelson, D. D., McManus, J. B., and Emmenegger, L.: High precision and continuous field measurements of $\delta^{13}C$ and $\delta^{18}O$ in carbon dioxide with a cryogen-free QCLAS, Appl. Phys. B, 92, 451–458, doi:10.1007/s00340-008-3085-4, 2008.

Tuzson, B., Hiller, R. V., Zeyer, K., Eugster, W., Neftel, A., Ammann, C., and Emmenegger, L.: Field intercomparison of two optical analyzers for CH_4 eddy covariance flux measurements, Atmos. Meas. Tech., 3, 1519–1531, doi:10.5194/amt-3-1519-2010, 2010.

Tuzson, B., Henne, S., Brunner, D., Steinbacher, M., Mohn, J., Buchmann, B., and Emmenegger, L.: Continuous isotopic composition measurements of tropospheric CO_2 at Jungfraujoch (3580 m a.s.l.), Switzerland: real-time observation of regional pollution events, Atmos. Chem. Phys., 11, 1685–1696, doi:10.5194/acp-11-1685-2011, 2011.

Volz-Thomas, A., Berg, M., Heil, T., Houben, N., Lerner, A., Petrick, W., Raak, D., and Pätz, H.-W.: Measurements of total odd nitrogen (NO_y) aboard MOZAIC in-service aircraft: instrument design, operation and performance, Atmos. Chem. Phys., 5, 583–595, doi:10.5194/acp-5-583-2005, 2005.

Werle, P.: Accuracy and precision of laser spectrometers for trace gas sensing in the presence of optical fringes and atmospheric turbulence, Appl. Phys. B, 102, 313–329, doi:10.1007/s00340-010-4165-9, 2011.

Werle, P., Mücke, R., and Slemr, F.: The limits of signal averaging in atmospheric trace-gas monitoring by tunable diode-laser absorption spectroscopy (TDLAS), Appl. Phys. B, 57, 131–139, doi:10.1007/BF00425997, 1993.

Wesely, M. L. and Hicks, B. B.: A review of the current status of knowledge on dry deposition, Atmos. Environ., 34, 2261–2282, doi:10.1016/S1352-2310(99)00467-7, 2000.

Zellweger, C., Ammann, M., Buchmann, B., Hofer, P., Lugauer, M., Rüttimann, R., Streit, N., Weingartner, E., and Baltensperger, U.: Summertime NO_y speciation at the Jungfraujoch, 3580 m above sea level, Switzerland, J. Geophys. Res.-Atmos., 105, 6655–6667, doi:10.1029/1999JD901126, 2000.

Zellweger, C., Forrer, J., Hofer, P., Nyeki, S., Schwarzenbach, B., Weingartner, E., Ammann, M., and Baltensperger, U.: Partitioning of reactive nitrogen (NO_y) and dependence on meteorological conditions in the lower free troposphere, Atmos. Chem. Phys., 3, 779–796, doi:10.5194/acp-3-779-2003, 2003.